1.05-GHz CMOS Oscillator Based on Lateral-Field-Excited Piezoelectric AlN Contour-Mode MEMS Resonators

Chengjie Zuo, *Student Member, IEEE*, Jan Van der Spiegel, *Fellow, IEEE*, and Gianluca Piazza, *Member, IEEE*

***Abstract*—This paper reports on the first demonstration of a 1.05-GHz microelectromechanical (MEMS) oscillator based on lateral-field-excited (LFE) piezoelectric AlN contour-mode resonators. The oscillator shows a phase noise level of −81 dBc/Hz at 1-kHz offset frequency and a phase noise floor of −146 dBc/Hz, which satisfies the global system for mobile communications (GSM) requirements for ultra-high frequency (UHF) local oscillators (LO). The circuit was fabricated in the AMI semiconductor (AMIS) 0.5-μm complementary metal-oxide-semiconductor (CMOS) process, with the oscillator core consuming only 3.5 mW DC power. The device overall performance has the best figure-of-merit (FoM) when compared with other gigahertz oscillators that are based on film bulk acoustic resonator (FBAR), surface acoustic wave (SAW), and CMOS on-chip inductor and capacitor (CMOS LC) technologies. A simple 2-mask process was used to fabricate the LFE AlN resonators operating between 843 MHz and 1.64 GHz with simultaneously high Q (up to 2,200) and k_t^2 (up to 1.2%). This process further relaxes manufacturing tolerances and improves yield. All these advantages make these devices suitable for post-CMOS integrated on-chip direct gigahertz frequency synthesis in reconfigurable multiband wireless communications.**

I. Introduction

Oscillator development based on microelectromechanical systems (MEMS) has drawn significant attention, because MEMS resonators can provide CMOS compatibility and multifrequency operation on a single chip [1], [2]. With either electrostatic [3], [4] or piezoelectric [5], [6] transduction, MEMS resonators have been recently demonstrated to attain simultaneously high quality factor ($Q > 1{,}000$) and high operating frequencies up to the gigahertz range. However, due to the relatively small electromechanical coupling coefficient ($k_t^2 < 0.6\%$) and thus large motional resistance, no gigahertz MEMS oscillator has been demonstrated using laterally vibrating resonators. The low coupling obtained to date combined with an increase in substrate parasitics and the need for higher power consumption when operating at higher frequencies [2] has in fact limited the demonstration of these oscillators.

Manuscript received May 19, 2009; accepted August 12, 2009. This work was supported by DARPA N/MEMS S&T grant no. HR-001-06-1-0041.

The authors are with the Department of Electrical and Systems Engineering, University of Pennsylvania, Philadelphia, PA (e-mail: czuo@seas.upenn.edu).

Digital Object Identifier 10.1109/TUFFC.1382

In the work reported in this paper, significant progress has been made toward the first demonstration of a 1.05-GHz oscillator based on lateral-field-excited (LFE) piezoelectric AlN contour-mode MEMS resonators (Fig. 1). By depositing a piezoelectric AlN layer directly on silicon wafers and making the film thickness, T, equal to approximately 0.45 times (which can be explained by Lamb wave theory [7]–[10] as it will be discussed in more details in the next section) the desired wavelength of operation, λ, both the material quality (therefore resonator Q) and k_t^2 have been optimized without being negatively affected by the quality of bottom metal films. In this way, simultaneous high Q (up to 2,200) and k_t^2 (up to 1.2%) have been achieved from 843 MHz to 1.64 GHz for LFE AlN resonators without a floating bottom electrode [5]. This solution makes the design of gigahertz MEMS oscillators with low power consumption possible. The demonstrated 1.05-GHz oscillator shows a phase noise of −81 dBc/Hz at 1-kHz offset frequency with a DC power consumption of 3.5 mW. The integrated circuit (IC) that is wire-bonded to the LFE AlN resonator was fabricated in the AMI semiconductor (AMIS) 0.5-μm CMOS process.

II. Piezoelectric LFE AlN Resonators

In our previous work, piezoelectric thickness-field-excited (TFE) AlN contour-mode resonators have been demonstrated to have high Q (up to 4000) in air, low motional resistance (~25 Ω), and multiple frequencies of operation [5], [11] on the same substrate. Based on a similar fabrication process, piezoelectric RF MEMS switches have been monolithically integrated with TFE AlN resonators [12]. TFE AlN resonators have also been used to demonstrate multifrequency oscillators (176–482 MHz) for next-generation reconfigurable frequency-reference and timing applications [2]. When the TFE scheme is pushed to higher frequencies (> gigahertz), the feature size of the electrodes decreases (gigahertz operation of AlN usually corresponds to a few microns for the lithographic patterning of electrodes), which poses a severe challenge for the microfabrication of these devices. The critical issues include degraded AlN deposition on densely patterned (due to uneven surface) wafers and high vulnerability to alignment errors.

Therefore, the idea of introducing LFE resonators without a floating bottom electrode is proposed to solve these

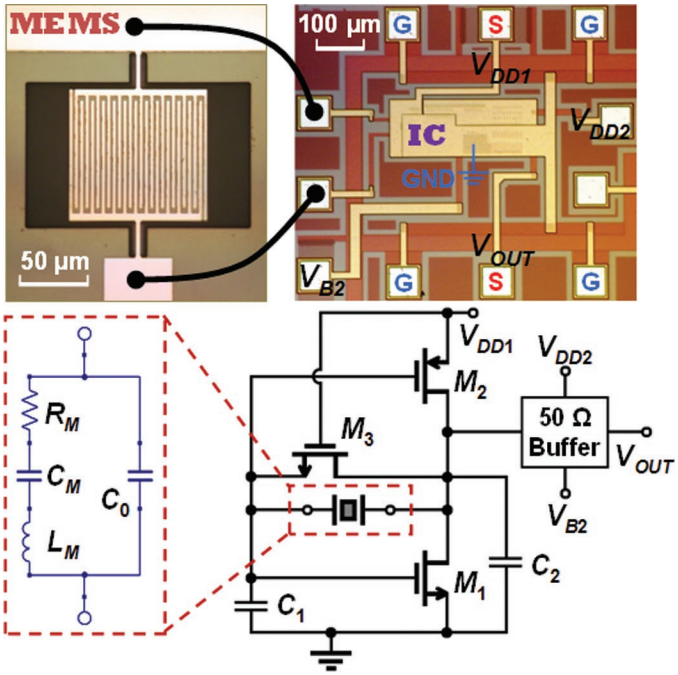

Fig. 1. Micrographs and circuit schematics of the 1.05-GHz LFE AlN MEMS resonator and its wire-bonding to the CMOS IC chip.

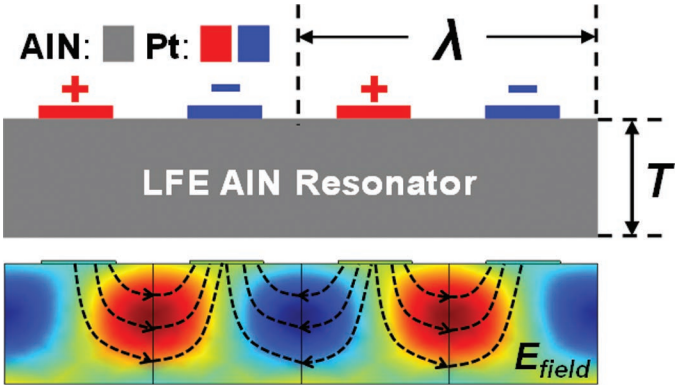

Fig. 2. Cross-sectional schematic and mode shape (displacement profile) of a piezoelectric LFE AlN contour-mode resonator.

problems. As shown in Fig. 2, LFE means that there are interdigitated metal electrodes only on top of the piezoelectric thin film, but not on the bottom side. The electric field has a laterally distributed component (perpendicular to the thickness direction), which is different than TFE AlN contour-mode MEMS resonators, whose electrical field is exclusively in the thickness direction. To avoid confusion between different "TFE" and "LFE" definitions in the ultrasonic community, it is important to note that the electrode configuration of the LFE AlN resonators of this work can also be described via the terminology used for the well-known interdigital transducer (IDT)–extensively studied for surface acoustic wave (SAW) excitation and recently studied [9], [10] for Lamb wave excitation in thin AlN films. Although K^2 has been traditionally used for describing the electromechanical coupling of LFE resonators [13], k_t^2, as employed for film bulk acoustic resonator (FBAR) [14], is adopted throughout this paper given K^2 is small and the 2 values do not differ significantly from a practical point of view.

By depositing AlN directly on low-roughness Si wafers, the AlN thin-film quality can be well controlled and optimized with current-day sputtering techniques. At the same time, misalignment errors are greatly relaxed, because only one top metal layer is needed to excite the resonator. Based on this LFE scheme, AlN resonators have been demonstrated up to 10 GHz with the highest $f{\cdot}Q$ product (~4.6×10^{12} Hz) ever reported for AlN contour-mode devices [6]. For oscillator applications, another important figure of merit (FoM) related to the resonator design is the $k_t^2{\cdot}Q$ product. Therefore, in addition to the quality factor optimization, the electromechanical coupling coefficient k_t^2 has been maximized in this work by making the film thickness T equal to about 0.45 times the desired wavelength of operation, λ, as illustrated in Fig. 2 [7]. In this way, simultaneous high Q (up to 2,200) and k_t^2 (up to 1.2%) have been achieved for LFE AlN resonators from 843 MHz to 1.64 GHz, as listed in Table I. The reason for this choice of film thickness mainly comes from the Lamb wave theory, where the maximum electromechanical coupling happens at 0.45λ for S_0 Lamb waves in AlN excited by IDT [7]–[10]. At this relatively large AlN thickness, the dispersion of the phase velocity deteriorates to a certain extent. Despite that, the frequency sensitivity to process variations (AlN thickness and electrode thickness) for LFE AlN contour-mode MEMS resonators is generally lower than (or at least comparable to) AlN FBAR resonators [7].

For the fabrication process (shown in Fig. 3), only 2 masks are needed: one for top electrode patterning and

TABLE I. EXPERIMENTAL RESULTS OF LFE ALN RESONATORS.

f_s [GHz]	Q_s	k_t^2	R_M [Ω]	λ [μm]	T [μm]
0.84	1900	0.67%	425	12	4
1.05	1450	1.20%	82	8	4
1.17	2200	0.96%	135	8	3
1.30	1700	0.80%	143	6	3
1.64	1450	0.39%	330	4	3

f_s = series resonant frequency; Q_s = quality factor at series resonance; k_t^2 = effective electromechanical coupling coefficient; R_M = motional resistance; λ = wavelength of operation; T = thickness of the AlN film. Note that experimental results for k_t^2 follow closely the trend of theoretical prediction, although some deviations from theory have been experienced due to fabrication inaccuracies and film deposition parameter variations.

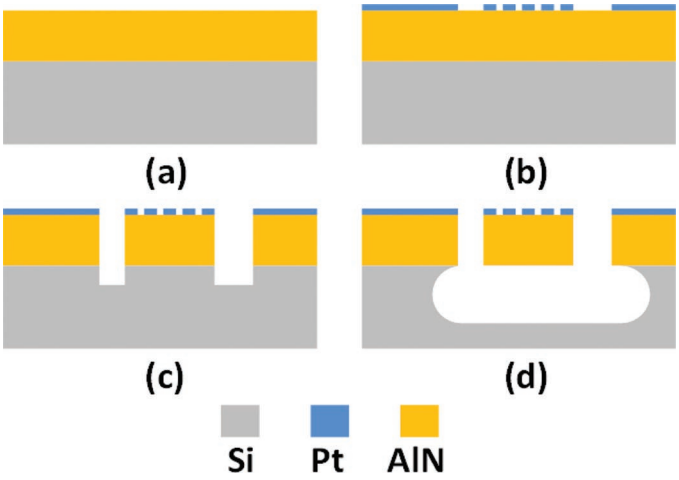

Fig. 3. Fabrication process: (a) direct AlN sputter deposition on top of Si wafers, (b) top Pt electrode deposition and patterning using lift-off, (c) AlN dry etching by inductively coupled plasma using Cl_2 and BCl_3, and (d) structure release by Si dry etching in XeF_2.

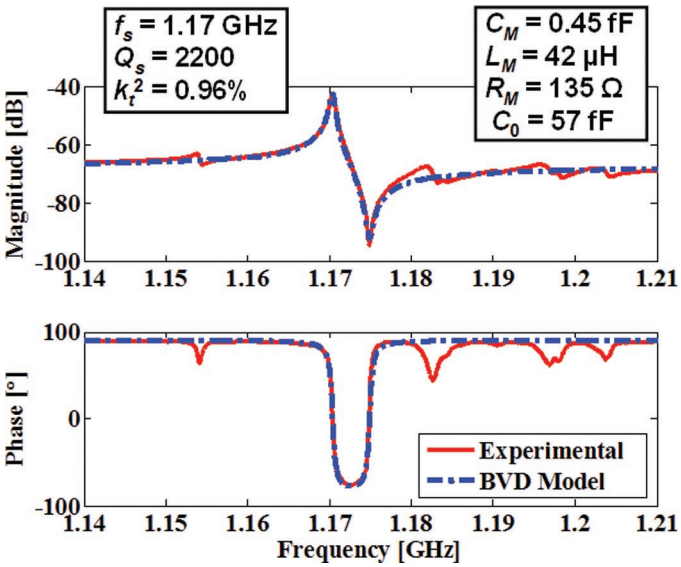

Fig. 4. Measured admittance plot and its BVD model fitting for a piezoelectric LFE AlN resonator at 1.17 GHz.

the other for AlN etching. Compared with the fabrication of TFE AlN resonators, the LFE scheme greatly reduces the number of steps, eliminates the bottom electrode deposition and the via definition (which has been a significant source of electrical resistance in TFE AlN resonators). Furthermore, due to the intrinsically lower k_t^2 of LFE (less than half of TFE) [7], the motional resistance of each of the subresonators (fingers) that form the device is higher than in TFE of comparable dimensions. Therefore, the overall device Q of LFE resonators is less influenced by the electrical loss in the metal electrodes or substrate parasitics. This aspect of LFE AlN resonators relaxes the stringent requirement on metal resistivity for conducting electrodes and reduces their impact on device Q. Considering all these aspects, Pt top electrodes have been chosen because high quality factors have been previously demonstrated with Pt electrodes in FBAR [15] and TFE AlN contour-mode resonators [2]. As an example of the resonator design (IDT transducer), the 1.05-GHz LFE resonator (Table I) has an AlN finger (sub-resonator [2]) width of 4 μm, a Pt electrode width of 2 μm (electrode coverage = 50%), an AlN finger length of 100 μm, and a total number of 26 fingers. The AlN thickness is 4 μm and the Pt thickness is 200 nm.

Similarly, because parasitic electrical loss is negligible for LFE AlN resonators, the traditional Butterworth-van Dyke (BVD) equivalent circuit model [14], instead of the modified-BVD model [2], has been adopted to describe the electrical performance, as shown in Fig. 1. As an example, the measured admittance plot (magnitude and phase), the BVD model fitting curve, and the equivalent circuit parameters of an LFE AlN resonator at 1.17 GHz are given in Fig. 4.

The power-handling capability of LFE resonators was also characterized. The electrical response of a 1.17-GHz device was measured for different driving power levels, and the magnitude of its admittance is plotted in Fig. 5. As we can see, the critical driving power before bifurcation occurs [16] is between 2 and 4 dBm, which roughly corresponds to a critical driving current of 3 mA. Compared with the 222-MHz TFE AlN resonator demonstrated earlier [2], this 1.17-GHz LFE AlN contour-mode resonator has a lower (about 1/3) current handling capability. The difference in power handling between the TFE and the LFE resonators is very specific to the 2 particular geometries and dimensions that are taken in consideration in this paper. The lower critical current can be primarily attributed to the relatively larger current-frequency effect (or amplitude-frequency effect characterized by the *A-f* coefficient, κ) of the 1.17-GHz resonator [16], which is also a function of the geometrical dimensions of the resonator. Therefore, the current-handling (power-handling) capability of LFE resonators is not necessarily lower than TFE resonators, and it can be properly designed to the required level by controlling the device geometry.

All the advantages, related to the elimination of the bottom metal layer deposition, flexibility in material selection (both the piezoelectric layer and conducting electrodes), fabrication simplicity, good power-handling capability, and high yield, make the LFE scheme extremely suitable for post-CMOS integration applications. The only trade-off consists in the limited frequency range in which the resonators exhibit a high electromechanical coupling, k_t^2, for a given thickness, T, of the piezoelectric material. Nevertheless, assuming a requirement of $k_t^2 > 1\%$, the available wavelength theoretically ranges between $T/0.6$ and $T/0.27$ [7], which corresponds to a useful frequency band equal to approximately 73% of the device center frequency for a given fixed film thickness, T.

III. Oscillator Circuit Design

The circuit topology adopted in this work and shown in Fig. 1 is similar to the Pierce oscillator presented in [2].

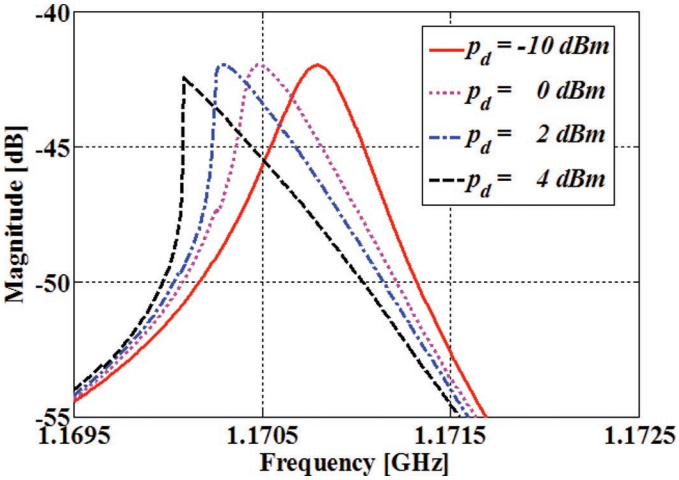

Fig. 5. Measured magnitude of admittance at different driving power levels, p_d, for the LFE AlN resonator at 1.17 GHz.

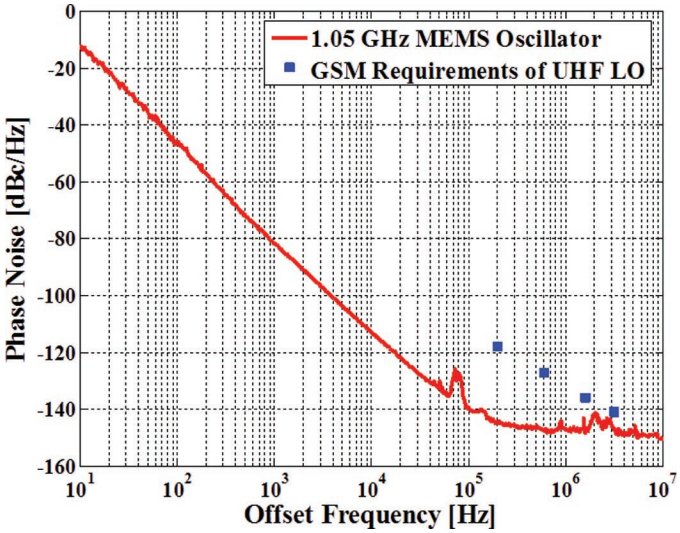

Fig. 6. Measured phase noise of the 1.05-GHz MEMS oscillator based on an LFE AlN resonator. The phase noise performance is compared with the GSM requirements of UHF LO.

The oscillator core is basically a CMOS-inverting amplifier formed by transistors M_1 and M_2 [17]. Transistor M_3 is biased to be always on and serves as a large resistor to bias the gate and drain voltages of transistors M_1 and M_2 at half V_{DD1}. This solution was implemented to minimize resistive loading on the resonator and maximize the allowable oscillating voltage swing. The DC bias current of M_1 is efficiently reused in M_2, so that the AC gain of the 2 transistors adds up. Except for having approximately twice the transconductance (g_m), the small-signal AC analysis of this oscillator core circuit is exactly the same as what has been shown in [2].

The novelty here consists in making possible the implementation of a tunable supply voltage (V_{DD1}) design, which is in line with the goal of having multifrequency resonators driven by the same oscillator core. For the oscillator circuit in Fig. 1, the total transconductance can be expressed as

$$\begin{aligned} g_m &= g_{m1} + g_{m2} \\ &\approx |\mu_n| C_{\text{ox}} \frac{W_1}{L_1}\left(\frac{V_{DD1}}{2} - |V_{\text{Tn}}|\right) \\ &\quad + |\mu_p| C_{\text{ox}} \frac{W_2}{L_2}\left(\frac{V_{DD1}}{2} - |V_{\text{Tp}}|\right), \end{aligned} \tag{1}$$

where μ_n is the electron mobility; μ_p is the hole mobility; C_{ox} is the capacitance per unit area of the gate oxide; V_{Tn} and V_{Tp} are the threshold voltages for N-type metal-oxide-semiconductor (NMOS) and P-type metal-oxide-semiconductor (PMOS) transistors, respectively; and W_1/L_1 and W_2/L_2 are the effective channel width-to-length ratios for the 2 transistors. From (1), we infer that the transconductance is linearly proportional to the supply voltage (V_{DD1}) for a fixed layout design. Therefore, the oscillator core proposed here (Fig. 1) can be effectively used as a tunable amplifier for the reconfigurable multifrequency oscillator (timing) solution proposed in our previous work [2], [18]. This solution allows us to optimize the oscillator gain (i.e., power consumption) for each specific frequency of operation of the resonators, instead of being forced to operate with a fixed gain set by the highest frequency of oscillation. By adjusting V_{DD1}, the DC bias current and, therefore, the AC gain in the circuit can be set to the point that is above the critical transconductance for the oscillations to start, so that both the phase noise performance and power consumption can be optimized for each switched-on resonator at a certain operating frequency. This capability is not experimentally proven in this paper, in which a single frequency oscillator is demonstrated, but is presented as a unique feature of this novel circuit topology and will be exploited in future implementations.

IV. Experimental Results

The AlN LFE resonators were fabricated with a 2-mask microfabrication process as shown in Fig. 3, while the tunable-supply-voltage oscillator circuit design was implemented in the AMIS 0.5-μm CMOS process. The MEMS resonator die was wire-bonded to the integrated circuit (IC) chip, and all other electrical contacts were made through the RF and DC probes available in the Desert Cryogenics TTP6 probe station (Desert Cryogenics, Tucson, AZ). The oscillator output was directly probed on chip and monitored via an Agilent E5052B Signal Source Analyzer (Agilent Technologies, Palo Alto, CA). As shown in Fig. 6, the measured phase noise of the 1.05-GHz MEMS oscillator for an output power of −23 dBm (limited by the current circuit design) is −81 dBc/Hz at 1-kHz offset frequency and as low as −146 dBc/Hz when the offset frequency is greater than 3×10^5 Hz. This phase noise performance already satisfies the stringent global system for mobile communications (GSM) requirements of ultra-high frequency (UHF) local oscillators (LO) [19]. Taking into

TABLE II. FoM Comparison of GHz Oscillators Based on Different Technologies.

Reference	f_o [GHz]	Phase noise [dBc/Hz]	P_{diss} [mW]	Technology	FoM [dBc/Hz]
This work 2009	1	−140 @ 100 kHz	3.5	AlN Contour-Mode MEMS 0.5 μm CMOS	−215
S. S. Rai 2008 [21]	2	−144 @ 1 MHz	0.6	FBAR 0.13 μm CMOS	−212
T. Sadek 2004 [22]	1	−156 @ 600 kHz	9.4	SAW 0.18 μm CMOS	−210
S. S. Rai 2008 [21]	2	−111 @ 1 MHz	0.6	LC VCO 0.13 μm CMOS	−180
J. Kim 2005 [20]	44	−101 @ 1 MHz	7.5	0.12 μm SOI CMOS	−185

account that the LFE AlN resonators have a power-handling capability much greater than −23 dBm, the phase noise floor can be further reduced if the oscillator circuit is designed to operate at a higher power level.

To compare the overall performance of different oscillators, a commonly used FoM has been established and is given by the following equation [20]:

$$\text{FoM} = L\left(f_m\right) - 20\log\left(\frac{f_o}{f_m}\right) + 10\log\left(\frac{P_{\text{diss}}}{1\ \text{mW}}\right), \quad (2)$$

where $L(f_m)$ is the oscillator phase noise at f_m, a specific offset frequency; f_o is the center frequency; P_{diss} is the DC power consumption (in milliwatts) of the oscillator circuit. The calculated FoM values for gigahertz oscillators based on different technologies are listed in Table II. As we can see, the 1.05-GHz MEMS oscillator demonstrated in this work has the best FoM when compared with other gigahertz oscillators based on FBAR, SAW, and CMOS on-chip inductor and capacitor (CMOS LC) technologies. In addition, the piezoelectric AlN contour-mode MEMS technology provides simultaneously multiple frequencies of operation on a single chip, CMOS compatibility, and high quality factor, whereas none of the other 3 technologies has all these combined capabilities.

By using this MEMS oscillator technology based on LFE piezoelectric AlN contour-mode resonators, multifrequency operation over a given frequency range can be realized with much better phase noise performance than conventional LC oscillators. With phase noise performance (of the free-running oscillator) further optimized to satisfy all the system-level requirements of different wireless standards, such as GSM, universal mobile telecommunications system (UMTS), and code division multiple access 2000 (CDMA2000), it is possible to envision the elimination of power-hungry phase-locked-loop (PLL) circuits for frequency synthesis in future single-chip and multiband reconfigurable transceiver solutions. In addition, the extended operating frequency range of these LFE AlN devices up to 10 GHz with high Q and low impedance makes possible the design of novel communication and sensing systems based on nontraditional RF architectures.

V. Conclusion

Design, fabrication, and testing of a 1.05-GHz CMOS oscillator based on LFE piezoelectric AlN contour-mode MEMS resonators have been demonstrated. This is the highest-frequency MEMS oscillator ever demonstrated using laterally vibrating resonators. The oscillator shows a phase noise of −81 dBc/Hz at 1-kHz offset frequency and a phase noise floor of −146 dBc/Hz, which satisfies the GSM requirements for UHF LO. The overall device performance has the best FoM when compared with other gigahertz oscillators that are based on FBAR, SAW, and CMOS LC technologies. The electromechanical coupling coefficient (k_t^2) for LFE resonators has been optimized to attain values up to 1.2% with simultaneously high Q (up to 2,200) in air. This was made possible by depositing AlN directly on Si wafers and making the film thickness equal to 0.45 times the desired wavelength of operation. In the future, we would like to expand this oscillator technology to microwave frequencies.

Acknowledgment

The authors thank N. Sinha for helping with Pt deposition. We also thank the MOSIS Educational Program for the IC chip fabrication and the staff at the Wolf Nanofabrication Facility at Penn for their support in the MEMS fabrication. Finally, AlN deposition has been performed by Tegal Corporation. The other members of the Penn Micro and Nano Systems Laboratory (PMaNS Lab) also deserve special thanks for valuable discussions and help.

References

[1] W.-T. Hsu, "Vibrating RF MEMS for timing and frequency references," presented at the IEEE MTT-S Int. Microwave Symp., San Francisco, CA, 2006, pp. 672–675.

[2] C. Zuo, N. Sinha, J. Van der Spiegel, and G. Piazza, "Multi-frequency pierce oscillators based on piezoelectric AlN contour-mode MEMS resonators," presented at the IEEE Int. Frequency Control Symp., Honolulu, HI, 2008, pp. 402–407.

[3] J. Wang, J. E. Butler, T. Feygelson, and C. T.-C. Nguyen, "1.51-GHz polydiamond micromechanical disk resonator with impedance-

mismatched isolating support," presented at the 17th IEEE Int. Micro Electro Mechanical Systems Conf. (MEMS 2004), Maastricht, The Netherlands, 2004, pp. 641–644.
[4] D. Weinstein and S. A. Bhave, "Internal dielectric transduction of a 4.5 GHz silicon bar resonator," presented at the Int. Electron Devices Meeting (IEDM 2007), Washington, DC, 2007, pp. 415–418.
[5] P. J. Stephanou and A. P. Pisano, "GHz contour extensional mode aluminum nitride MEMS resonators," presented at the IEEE Int. Ultrasonics Sym., Vancouver, Canada, 2006, pp. 2401–2404.
[6] M. Rinaldi, C. Zuniga, and G. Piazza, "5–10 GHz AlN contour-mode nanoelectromechanical resonators," presented at the 22nd IEEE Int. Conf. Micro Electro Mechanical Systems (MEMS 2009), Sorrento, Italy, 2009, pp. 916–919.
[7] J. H. Kuypers, C.-M. Lin, G. Vigevani, and A. P. Pisano, "Intrinsic temperature compensation of aluminum nitride lamb wave resonators for multiple-frequency references," presented at the IEEE Int. Frequency Control Symp., Honolulu, HI, 2008, pp. 240–249.
[8] A. Volatier, G. Caruyer, D. P. Tanon, P. Ancey, and E. Defaÿ, "UHF/VHF resonators using lamb waves co-integrated with bulk acoustic wave resonators," presented at the IEEE Int. Ultrasonics Symp., Rotterdam, The Netherlands, 2005, vol. 2, pp. 902–905.
[9] V. Yantchev and I. Katardjiev, "Micromachined thin film plate acoustic resonators utilizing the lowest order symmetric lamb wave mode," *IEEE Trans. Ultrason. Ferroelectr. Freq. Control*, vol. 54, no. 1, pp. 87–95, Jan. 2007.
[10] V. Yantchev and I. Katardjiev, "Thin AlN film resonators utilizing the lowest order symmetric Lamb mode: Further developments," presented at the European Frequency and Time Forum and IEEE Frequency Control Symp., Geneva, Switzerland, 2007, pp. 1067–1072.
[11] G. Piazza, P. J. Stephanou, and A. P. Pisano, "Piezoelectric aluminum nitride vibrating contour-mode MEMS resonators," *J. Microelectromech. Syst.*, vol. 15, no. 6, pp. 1406–1418, 2006.
[12] N. Sinha, R. Mahameed, C. Zuo, M. B. Pisani, C. R. Perez, and G. Piazza, "Dual-beam actuation of piezoelectric AlN RF MEMS switches monolithically integrated with AlN contour-mode resonators," in *Solid State Sensor, Actuator and Microsystems Workshop*, Hilton Head, SC, 2008, pp. 22–25.
[13] J. F. Rosenbaum, *Bulk Acoustic Wave Theory and Devices*. Norwood, MA: Artech House, 1988.
[14] J. D. Larson, III, P. D. Bradley, S. Wartenberg, and R. C. Ruby, "Modified Butterworth-Van Dyke circuit for FBAR resonators and automated measurement system," in *Proc. IEEE Ultrasonics Symp.*, 2000, vol. 1, pp. 863–868.
[15] C.-H. Lin, H.-R. Chen, and W. Fang, "Design and fabrication of a miniaturized bulk acoustic filter by high aspect ratio etching," *J. Micro/Nanolithography, MEMS, and MOEMS*, vol. 4, no. 3, art. no., 033010, 2005.
[16] V. Kaajakari, T. Mattila, A. Oja, and H. Seppa, "Nonlinear limits for single-crystal silicon microresonators," *J. Microelectromech. Syst.*, vol. 13, no. 5, pp. 715–724, 2004.
[17] Y. H. Chee, A. M. Niknejad, and J. Rabaey, "A sub-100μW 1.9-GHz CMOS oscillator using FBAR resonator," in *IEEE Radio Frequency Integrated Circuits Symp.*, Long Beach, CA, 2005, pp. 123–126.
[18] G. Piazza, P. J. Stephanou, and A. P. Pisano, "One and two port piezoelectric higher order contour-mode MEMS resonators for mechanical signal processing," *Solid-State Electron.*, vol. 51, no. 11-12, pp. 1596–1608, 2007.
[19] Q. Gu, *RF System Design of Transceivers for Wireless Communications*. New York: Springer, 2005.
[20] J. Kim, J.-O. Plouchart, N. Zamdmer, R. Trzcinski, K. Wu, B. J. Gross, and M. Kim, "A 44 GHz differentially tuned VCO with 4 GHz tuning range in 0.12 μm SOI CMOS," in *IEEE Int. Solid-State Circuits Conf.*, San Francisco, CA, 2005, vol. 1, pp. 416–417.
[21] S. S. Rai and B. P. Otis, "A 600 μW BAW-tuned quadrature VCO using source degenerated coupling," *IEEE J. Solid State Circuits*, vol. 43, no. 1, pp. 300–305, 2008.
[22] T. Sadek and P. M. Smith, "Low voltage SAW oscillator," in *Canadian Conf. Electrical and Computer Engineering*, Niagara Falls, Ontario, Canada, 2004, vol. 1, pp. 117–120.

Chengjie Zuo (S'07) received his B.S. degree in electronic information science and technology from the University of Science and Technology of China (USTC), Hefei, Anhui, China, in 2004 and M.Sc. degree in electrical engineering with honors from the Delft University of Technology (TU Delft), Delft, The Netherlands, in 2006. He is currently working toward his Ph.D. degree in electrical and systems engineering at the University of Pennsylvania, Philadelphia, PA. His research interests primarily include micro/nano electromechanical systems (MEMS/NEMS) devices, analog and RF integrated circuits (IC), and MEMS-IC integration and co-design. He is a student member of IEEE.

Jan Van der Spiegel (S'73–M'79–SM'90–F'02) received his M.S. and Ph.D. degrees in electrical engineering from the University of Leuven, Belgium, in 1974 and 1979, respectively.

He joined the University of Pennsylvania, Philadelphia, PA, in 1981 where he is currently a professor in the Department of Electrical and Systems Engineering and the director of the Center for Sensor Technologies. His research interests are in mixed-mode VLSI design, biologically based sensors and sensory information processing systems, micro-sensor technology, and analog-to-digital converters.

Dr. Van der Spiegel is a fellow of the IEEE (2002) and the recipient of the IEEE Educational Activities Board Major Educational Innovation Award (2007), the IEEE Third Millennium Medal (2000), the UPS Foundation Distinguished Education Chair, and the Bicentennial Class of 1940 Term Chair. He received the Christian and Mary Lindback Foundation and the S. Reid Warren Award for Distinguished Teaching.

Dr. Van der Spiegel has served on several IEEE program committees and was the program chair of the 2007 International Solid-State Circuit Conference (ISSCC). He has been the chapters' chairs coordinator of the IEEE Solid-State Circuits Society (SSCS). He is an elected member of SSCS, a Distinguished Lecturer of the SSCS, and a member of the SSCS membership committee.

Gianluca Piazza (S'00–M'05) is a Wilf Family Term Assistant Professor in the Department of Electrical and Systems Engineering (ESE) at the University of Pennsylvania, Philadelphia, PA. His research interests focus on piezoelectric micro and nano systems (MEMS/NEMS) for RF wireless communications, biological detection, wireless sensor platforms, and all mechanical computing. He also has general interest in the areas of micro/nano fabrication techniques and integration of micro/nano devices with state-of-the-art electronics. He received his Ph.D. degree from the University of California, Berkeley, where he developed a new class of AlN contour-mode vibrating microstructures for RF communications. He has more than 10 years of experience working with piezoelectric materials. He holds two patents in the field of micromechanical resonators and has recently co-founded a start-up (Harmonic Devices, Inc.) aiming at the commercialization of single-chip and multiband RF filters and oscillators. He received the IBM Young Faculty Award in 2006 and has won, with his students, the Best Paper Award in Group 1 and 2 at the IEEE Frequency Control Symposium in 2008 and 2009, respectively.